Quantitative Finance
Publication details, including instructions for authors and subscription information:
http://www.tandfonline.com/loi/rquf20

Multiscale analysis of economic time series by scale-dependent Lyapunov exponent

Jianbo Gao [a], Jing Hu [b], Wen-Wen Tung [c] & Yi Zheng [d]

[a] PMB Intelligence LLC, PO Box 2077, West Lafayette, IN 47996, USA

[b] Affymetrix, Inc., 3380 Central Expressway, Santa Clara, CA 95051, USA

[c] Department of Earth & Atmospheric Sciences, Purdue University, West Lafayette, IN 47907, USA

[d] Kellogg Group, LLC, 55 Broadway, 4th Floor, New York, NY 10006, USA

Available online: 10 Aug 2011

To cite this article: Jianbo Gao, Jing Hu, Wen-Wen Tung & Yi Zheng (2011): Multiscale analysis of economic time series by scale-dependent Lyapunov exponent, Quantitative Finance, DOI:10.1080/14697688.2011.580774

To link to this article: http://dx.doi.org/10.1080/14697688.2011.580774

Quantitative Finance, 2011, 1–10, iFirst

Multiscale analysis of economic time series by scale-dependent Lyapunov exponent

JIANBO GAO*†, JING HU‡, WEN-WEN TUNG§ and YI ZHENG¶

†PMB Intelligence LLC, PO Box 2077, West Lafayette, IN 47996, USA
‡Affymetrix, Inc., 3380 Central Expressway, Santa Clara, CA 95051, USA
§Department of Earth & Atmospheric Sciences, Purdue University, West Lafayette, IN 47907, USA
¶Kellogg Group, LLC, 55 Broadway, 4th Floor, New York, NY 10006, USA

(*Received 13 May 2009; in final form 11 April 2011*)

Economic time series usually exhibit complex behavior such as nonlinearity, fractal long-memory, and non-stationarity. Recently, considerable efforts have been made to detect chaos and fractal long-memory in finance. While evidence supporting fractal scaling in finance has been accumulating, it is now generally thought that financial time series may not be modeled by chaos or noisy chaos, since the estimated Lyapunov exponent (LE) is negative. A negative LE amounts to a negative Kolmogorov entropy, and thus implies simple regular dynamics of the economy. This is at odds with the general observation that the economy is highly complicated due to nonlinear and stochastic interactions among component systems and hierarchical regulations in the world economy. To resolve this dilemma, and to provide an effective means of characterizing fractal long-memory properties in non-stationary economic time series, we employ a multiscale complexity measure, the scale-dependent Lyapunov exponent (SDLE), to characterize economic time series. SDLE cannot only unambiguously distinguish low-dimensional chaos from noise, but also detect high-dimensional and intermittent chaos, as well as effectively deal with non-stationarity. With SDLE, we are able to show that the reported negative LE may correspond to large-scale convergence, but not imply the absence of small-scale divergence or noisy chaos in the world economy. Using US foreign exchange rate data as examples, we further show how SDLE can readily characterize fractal, persistent or anti-persistent long-range correlations in economic time series.

Keywords: Nonlinear dynamics; Financial time series; Long memory volatility processes; Power law correlation

JEL Classification: C1, C2, C14, C22

1. Introduction

Economic time series are highly irregular. They often exhibit complex characteristics such as nonlinearity, fractal long-memory, and non-stationarity. In the past two decades, considerable efforts have been made to detect chaos (Barnett and Chen 1988, Brock and Sayers 1988, Scheinkman and LeBaron 1989, Granger 1991, 1994, Barnett *et al*. 1997, Whang and Linton 1999, Wesner 2004, Barnett 2006, Kyrtsou and Serletis 2006, Serletis and Shintani 2006), and fractal, multifractal, and long-memory (Granger and Ding 1996, Breidt *et al*. 1998, Dacorogna *et al*. 2001, Zumbach 2004, Oswiecimka *et al*. 2005, Di Matteo 2007, Mcmillan and Speigh 2008) in finance. While recent works have suggested the existence of fractal, multifractal, and long-memory behavior in finance (Dacorogna *et al*. 2001, Zumbach 2004, Oswiecimka *et al*. 2005, Di Matteo 2007, Mcmillan and Speigh 2008), it is now generally believed that economic time series may not be modeled by deterministic chaos or noisy low-dimensional chaos (Barnett 2006, Serletis and Shintani 2006). The conclusion concerning the irrelevance of low-dimensional chaos was reached based on a negative value of a neural-network-based Lyapunov exponent (LE) estimator (Shintani and Linton 2003, 2004, Hommes and Manzan 2006). While the conclusion is as one would have anticipated, the reasoning is questionable, because of the

*Corresponding author. Email: jbgao@pmbintelligence.com

Quantitative Finance
ISSN 1469–7688 print/ISSN 1469–7696 online © 2011 Taylor & Francis
http://www.informaworld.com
DOI: 10.1080/14697688.2011.580774

following considerations. The sum of the positive LEs gives a tight upper bound to the Kolmogorov–Sinai (KS) entropy (Pesin 1977, Ruelle 1978). The KS entropy characterizes the rate of creation of information in a dynamic system. It is zero, positive, and infinite for regular, chaotic, and random dynamics, respectively (Grassberger and Procaccia 1983a,b). Therefore, a negative largest LE in economic time series amounts to a negative KS entropy, and thus implies regular economic dynamics. This is at odds with the general observation that the economy is anything but simple! To resolve this dilemma in general and how negative Lyapunov exponents could emerge from noisy chaotic finance models in particular, and equally importantly to provide a new means of characterizing fractal, long-memory properties in (possibly non-stationary) financial time series, in this study we employ a multiscale complexity measure, the scale-dependent Lyapunov exponent (SDLE) (Gao *et al.* 2006b, 2007), to examine a chaotic asset pricing model driven by dynamic noise (Brock and Hommes 1998), as well as a number of US foreign exchange rate data.

The remainder of the paper is organized as follows. In section 2 we describe the SDLE and study its properties that are most relevant to economic time series analysis. In section 3 we use the SDLE to analyse a chaotic asset pricing model driven by dynamic noise (Brock and Hommes 1998), as well as a number of US foreign exchange rate data. In section 4 we make a few concluding remarks.

2. SDLE as a multiscale complexity measure

2.1. SDLE: Definition and computation

SDLE is defined in a phase space by the consideration of an ensemble of trajectories (Gao *et al.* 2006b, 2007). In the case of a scalar time series $x(1), x(2), \ldots, x(n)$, a suitable phase space may be obtained by using time delay embedding (Packard *et al.* 1980, Takens 1981, Sauer *et al.* 1991) to construct vectors of the form

$$V_i = [x(i), x(i+L), \ldots, x(i+(m-1)L)], \tag{1}$$

where m and L are called the embedding dimension and the delay time, respectively. For chaotic systems, m and L have to be chosen according to certain optimization criteria (Gao *et al.* 2007). For a stochastic process, which is infinite-dimensional, the embedding procedure transforms a self-affine stochastic process into a self-similar process in a phase space, and often $m=2$ is sufficient (this issue will be explained further below) (Gao *et al.* 2006b, 2007).

We will now be more concrete. Denote the initial distance between two nearby trajectories by ϵ_0 and their *average distances* at time t and $t+\Delta t$, respectively, by ϵ_t and $\epsilon_{t+\Delta t}$, where Δt is small. The SDLE $\lambda(\epsilon_t)$ is defined by (Gao *et al.* 2006b, 2007)

$$\epsilon_{t+\Delta t} = \epsilon_t \mathrm{e}^{\lambda(\epsilon_t)\Delta t} \quad \text{or} \quad \lambda(\epsilon_t) = \frac{\ln \epsilon_{t+\Delta t} - \ln \epsilon_t}{\Delta t}, \tag{2}$$

or, equivalently, by

$$\frac{\mathrm{d}\epsilon_t}{\mathrm{d}t} = \lambda(\epsilon_t)\epsilon_t \quad \text{or} \quad \frac{\mathrm{d}\ln \epsilon_t}{\mathrm{d}t} = \lambda(\epsilon_t). \tag{3}$$

To compute the SDLE, we can start from an arbitrary number of shells,

$$\epsilon_k \le \|V_i - V_j\| \le \epsilon_k + \Delta\epsilon_k, \quad k = 1, 2, 3, \ldots, \tag{4}$$

where V_i and V_j are reconstructed vectors, and ϵ_k (the radius of the shell) and $\Delta\epsilon_k$ (the width of the shell) are arbitrarily chosen small distances ($\Delta\epsilon_k$ is not necessarily a constant). Then we monitor the evolution of all pairs of points (V_i, V_j) within a shell and take the average. Equation (2) can now be written as

$$\lambda(\epsilon_t) = \frac{\langle \ln \|V_{i+t+\Delta t} - V_{j+t+\Delta t}\| - \ln \|V_{i+t} - V_{j+t}\| \rangle}{\Delta t}, \tag{5}$$

where t and Δt are integers in units of the sampling time, and the angled brackets denote the average within a shell. Note that this computational procedure is similar to that for computing the so-called time-dependent exponent curves (Gao and Zheng 1994).

Note that the initial set of shells serve as initial values of the scales; by evolution of the dynamics, they will automatically converge to the range of inherent scales. This is emphasized by the subscript t in ϵ_t—when the scales become inherent, t can then be dropped. Also note that when analysing chaotic time series, the condition

$$|j - i| \ge (m-1)L \tag{6}$$

needs to be imposed when finding pairs of vectors within a shell in order to eliminate the effects of tangential motion (Gao *et al.* 2007). This condition is often also sufficient for an initial scale to converge to the inherent scales (Gao *et al.* 2007).

To better understand SDLE, it is instructive to point out a relation between SDLE and the largest positive Lyapunov exponent λ_1 for true chaotic signals. This is given by (Gao *et al.*, 2007)

$$\lambda_1 = \int_0^{\epsilon^*} \lambda(\epsilon)\, p(\epsilon) \mathrm{d}\epsilon, \tag{7}$$

where ϵ^* is a scale parameter (for example, used for re-normalization when using the algorithm of Wolf *et al.* (1985)), $p(\epsilon)$ is the probability density function for the scale ϵ given by

$$p(\epsilon) = Z \frac{\mathrm{d}C(\epsilon)}{\mathrm{d}\epsilon}, \tag{8}$$

where Z is a normalization constant ensuring $\int_0^{\epsilon^*} p(\epsilon) \times \mathrm{d}\epsilon = 1$, and $C(\epsilon)$ is the well-known Grassberger–Procaccia's correlation integral (Grassberger and Procaccia 1983b).

SDLE has distinctive scaling laws for different types of time series. Those most relevant to economic time series analysis are listed here.

(1) For clean chaos on small scales, and noisy chaos with weak noise on intermediate scales,

$$\lambda(\epsilon) = \lambda_1. \tag{9}$$

As an operational definition for chaos, we define chaos to be observing the scaling of equation (9) on a scale range of $(\epsilon, r\epsilon)$, where $r>1$ is a coefficient (Gao *et al.* 2006b, 2007). Where low-dimensional chaos is concerned, one may require $r \geq 2$.

(2) For clean chaos on large scales where memory has been lost and for noisy chaos (including noise-induced chaos (Gao *et al.* 1999a,b, Hwang *et al.* 2000)) on small scales,

$$\lambda(\epsilon) \sim -\gamma \ln \epsilon, \tag{10}$$

where $\gamma>0$ is a parameter. Recently, using an ensemble forecasting approach, we have proven (but not yet published) that $\gamma = D/D(\epsilon_0)$, where D and $D(\epsilon_0)$ are the information dimension on the infinitesimal and an initial finite scale in ensemble forecasting. When a noisy dataset is finite, due to lack of data, D would soon saturate when m exceeded a certain value. However, if the finite scale is quite large, $D(\epsilon_0) \sim m$, for a wide range of m, yielding $\gamma \sim 1/m$. This also implies that when m is too large, it becomes difficult to observe the scaling of equation (10). Therefore, $m=2$ is preferred.

(3) For random $1/f^{2H+1}$ processes, where $0<H<1$ is called the Hurst parameter which characterizes the correlation structure of the 'increment' of the process: depending on whether H is smaller than, equal to, or larger than 1/2, the increment of the process is said to have anti-persistent, short-range, or persistent long-range correlations (Gao *et al.* 2006c, 2007),

$$\lambda(\epsilon) \sim \epsilon^{-1/H}. \tag{11}$$

Note that $H=1/2$ for standard Brownian motion and $H=1/3$ for turbulence. Note also that this scaling is quite independent of m, except that the scale range defining equation (11) shrinks when m increases. Because of this, $m=2$ is again preferred.

2.2. Detecting high-dimensional chaos

In order to unambiguously determine whether an economic time series can be modeled by chaos or noisy chaos, it is important to clearly understand whether SDLE can detect chaos in a system with multiple positive Lyapunov exponents. For this purpose, we study the Lorenz '96 model (Lorenz 1996, 2005, Lorenz and Emanuel 1998). The model is assumed to represent some atmospheric quantity equally spaced around a latitudinal circle. It is described by the following equation:

$$\mathrm{d}X_n/\mathrm{d}t = (X_{n+1} - X_{n-2})X_{n-1} - X_n + F, \quad n = 1, 2, \ldots, N, \tag{12}$$

with periodic boundary condition, i.e. $X_{-1} = X_{N-1}$, $X_0 = X_N$, and $X_{N+1} = X_1$. F is a positive constant representing external forcing. The term $-X_n$ represents dissipation, and the term $(X_{n+1} - X_{n-2})\ X_{n-1}$ represents advection. When $N=40$ and $F=8$, the system has 13 positive Lyapunov exponents and a Kaplan–Yorke dimension of 27.1. In the ensemble forecasting of this system, one chooses many points in a small neighborhood of a reference point, integrates the system starting from all those points, and monitors the divergence between all those perturbed trajectories and the reference trajectory. The average of this divergence is called the error growth curve. Since this system is chaotic, initially the error grows exponentially, or linearly on a semi-log plot. The rate of growth gives the largest positive LE. This behavior is shown as the blue curve in figure 1(a). Because of the high dimension here, the scale range of observing $\lambda(\epsilon) \sim$ constant is very narrow, as shown in figure 1(b). Nevertheless, the pattern of SDLE clearly indicates deterministic chaos. In fact, the integration of $\lambda(\epsilon) \sim$ gives the solid red curve in figure 1(a), which collapses on the blue error growth curve from ensemble forecasting. The dashed red curve, which is obtained by linearly extrapolating the solid red curve, together with the solid red curve, perfectly recovers the blue error growth curve from ensemble forecasting. Therefore, we can conclude that SDLE can readily detect high-dimensional deterministic chaos.

2.3. Detecting intermittent chaos

In science and engineering, an important type of complex motion is intermittent chaos, a type of motion that is characterized by a long laminar phase during which neighboring trajectories do not diverge, and a rapid divergence over a small part of the state space. Existing

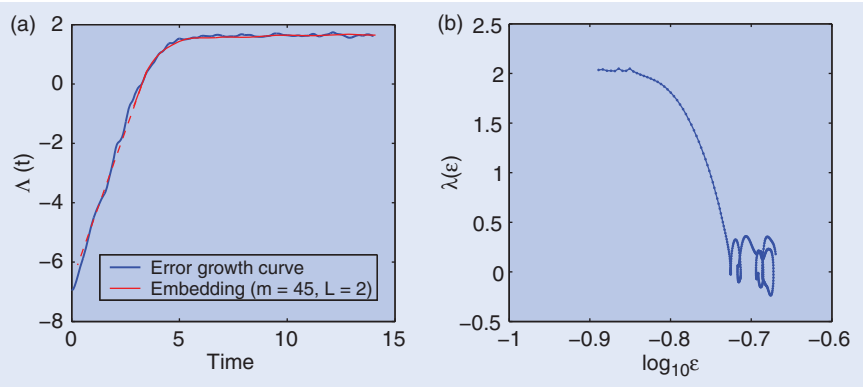

Figure 1. (a) Error growth curves for the Lorenz '96 system, where $\Lambda(t)$ is the logarithm of the root mean square error. The blue curve is the average of the error curves of 250 ensembles, and the red curve is the integration of SDLE (the dashed part of the red curve represents a linear extrapolation of the solid red curve). (b) The $\lambda(\epsilon)$ curve based on X_1 time series of the Lorenz '96 system.

methods for detecting chaos cannot deal with such a situation, since the long laminar phase would dominate, yielding only a zero Lyapunov exponent. However, SDLE can readily indicate chaos even in such a situation. To show this, we study the logistic map

$$x_{n+1} = ax_n(1 - x_n), \quad a = 3.8284. \tag{13}$$

Figure 2(a) shows an intermittent time series. We note that the chaotic part is very short compared with the periodic part. Figure 2(b) shows the SDLE curve for the time series. We clearly observe a plateau defining chaotic motion. Also note that the ln ϵ scaling on very small scales indicates the transitions from periodic to chaotic motion, and *vice versa* (it is unstable, but not chaotic in the rigorous sense).

2.4. *Coping with non-stationarity*

Since economic time series may be non-stationary, it is important to understand how SDLE deals with non-stationarity before it is used to analyse financial data. Noting that fractal $1/f$ scaling behavior has been observed in finance (Dacorogna *et al.* 2001, Zumbach 2004, Oswiecimka *et al.* 2005, Di Matteo 2007, Mcmillan and Speigh 2008), we first study if the $1/f$ feature remains robust under the following perturbations.

(1) Shift a $1/f^{\beta}$, $\beta = 2H + 1$ process downward or upward at randomly chosen points in time by an arbitrary amount. For convenience, we call this procedure type-1 non-stationarity and the processes obtained broken-$1/f^{\beta}$ processes.
(2) At randomly chosen time intervals, concatenate randomly broken-$1/f^{\beta}$ processes and oscillatory components or superimpose oscillatory components on broken-$1/f^{\beta}$ processes. This procedure causes a different type of non-stationarity, which, for convenience, we shall call type-2 non-stationarity.

We call the resulting random processes perturbed $1/f^{\beta}$ processes. Three examples of the $\lambda(\epsilon)$ curves for such processes, where the frequency of the perturbations are, on average, 1% of the simulated data, are shown in figure 3(b). Compared with the SDLE curves for the unperturbed $1/f$ processes shown in figure 3(a), we conclude that equation (11) still holds very well when $\lambda(\epsilon) > 0.02$. Therefore, SDLE can readily characterize $1/f$ processes perturbed by either of the non-stationarities considered.

To understand why the SDLE can deal with type-1 non-stationarity, it suffices to note that type-1 non-stationarity causes shifts of the trajectory in phase space; the greater the non-stationarity, the larger the shifts. The SDLE, however, is not affected much by shifts, especially large ones, since it is based on the co-evolution of pairs of vectors within chosen small shells. In fact, the effect of shifts is to exclude a few pairs of vectors that were originally counted in the ensemble average. Therefore, as long as the shifts are not too frequent, the effect of shifts can be neglected, since the ensemble average within a shell involves a large number of pairs of vectors.

Let us now turn to type-2 non-stationarity, which involves oscillatory components. Being regular,

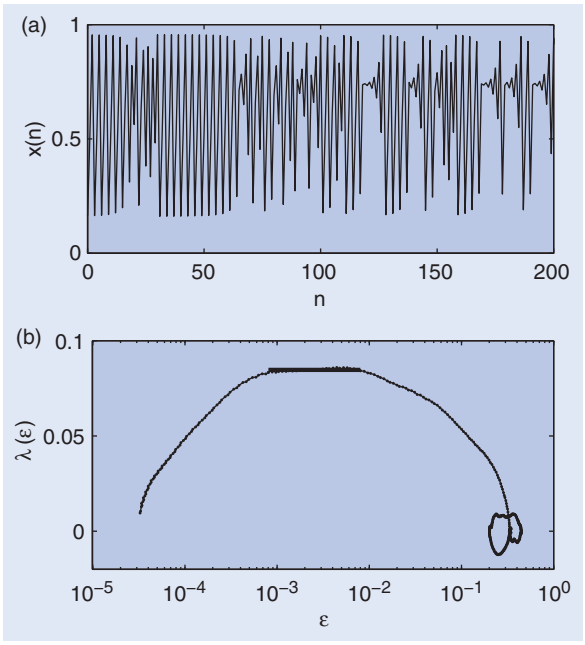

Figure 2. (a) An intermittent time series generated by the logistic map. (b) The SDLE curve for the time series.

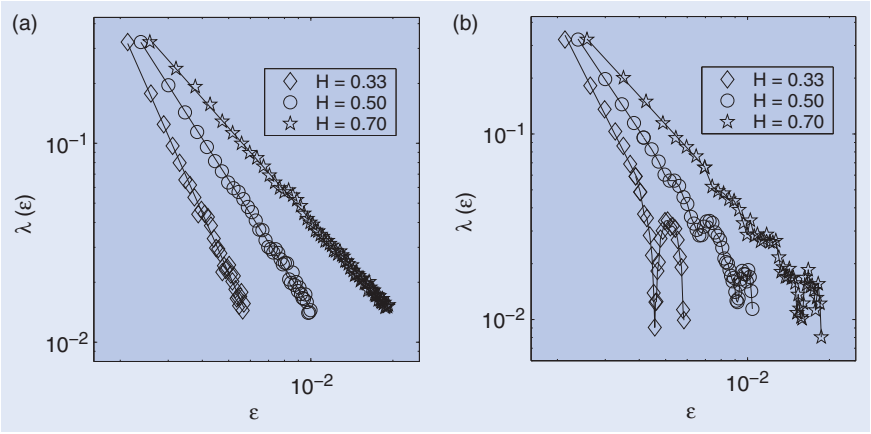

Figure 3. $\lambda(\epsilon)$ curves for (a) $1/f^{2H+1}$ processes with $H = 1/3$, 0.5, and 0.7 and (b) perturbed $1/f^{2H+1}$ processes.

oscillatory components can only affect $\lambda(\epsilon)$ where it is close to 0. Therefore, type-2 non-stationarity does not affect the positive portion of $\lambda(\epsilon)$ either.

We have carried out similar perturbations to chaotic and noisy chaotic data. The major features of equations (9) and (10) are also robust, as expected. In fact, intermittent chaos studied in section 2.3 may be viewed as a variant of such perturbations. Therefore, we conclude that SDLE can readily deal with non-stationarity.

Finally, we note that the fractal scalings of perturbed $1/f$ processes cannot be well characterized by other approaches, such as fluctuation analysis, rescaled range analysis, detrended fluctuation analysis, etc. (Gao *et al.* 2006c, 2007).

3. Analysis of economic time series

In this section, we first examine how negative Lyapunove exponents could emerge from noisy chaotic finance models when noise is increased, and then carry out SDLE analysis of a number of US foreign exchange rate data. The first task will be achieved by studying a chaotic asset pricing model with heterogeneous beliefs driven by dynamic noise proposed by Brock and Hommes (1998).

3.1. Analysis of a chaotic asset pricing model

The chaotic asset pricing model with heterogeneous beliefs driven by dynamic noise proposed by Brock and Hommes (1998) is a nonlinear map of the form

$$x_t = F(x_{t-1}, x_{t-2}, x_{t-3}) + \sigma\eta_t. \tag{14}$$

Specifically, the model is described by the following equations:

$$x_t = \frac{1}{R}\sum_{h=1}^{4} n_{h,t}(g_h x_{t-1} + b_h) + \sigma\eta_t, \tag{15}$$

$$n_{h,t} = \frac{e^{\beta U_{ht-1}}}{\sum_{j=1}^{4} e^{\beta U_{jt-1}}}, \tag{16}$$

$$U_{h,t-1} = (x_{t-1} - Rx_{t-2})(g_h x_{t-3} + b_h - Rx_{t-2}). \tag{17}$$

Here x_t denotes the deviation of the price of the risky asset from its benchmark fundamental value (the discounted sum of expected future dividends), $R>1$ is the constant risk-free rate, $n_{h,t}$ represents the discrete choice of agents using belief type h, $U_{h,t-1}$ is the profit generated by strategy h in the previous period, g_h and b_h characterize the linear belief with one time lag of strategy h, and the noise term $\sigma\eta_t$ is standard normally distributed with variance σ^2. For suitable choices of the parameter values, the model exhibits chaotic dynamics. In particular, Brock and Hommes studied the model with parameter values $\beta=90, R=1.1, g_1=b_1=0, g_2=1.1, b_2=0.2, g_3=0.9, b_3=-0.2, g_4=1.21, b_4=0$. They found that the motion is chaotic with the largest Lyapunov exponent 0.1. More recently, Hommes and Manzan (2006) studied the model with parameter values $\beta=90, R=1.01, g_1=b_1=0, g_2=0.9, b_2=0.2, g_3=0.9, b_3=-0.2, g_4=1.01, b_4=0$. When $\sigma=0$, they found that the motion is chaotic with the largest Lyapunov exponent around 0.135. When σ is increased beyond 0.1, they found that the largest Lyapunov exponent becomes negative. Here, we shall focus on these two parameter sets. For convenience, we call them the BH and the HM parameter set, respectively.

We have calculated the $\lambda(\epsilon)$ curves for the model with the BH and HM parameter set for various levels of noise. The results are shown in figures 4(a) and (b). We observe a few interesting features. (i) For the clean chaotic signal, when ϵ is smaller than a threshold value (which is determined by the size of the chaotic attractor), $\lambda(\epsilon)$ slightly fluctuates around a constant. As can be readily understood, this constant is the very largest positive LE. The value of about 0.1 shown in figure 4(b) is consistent with the LE obtained by Brock and Hommes (1998), but the value of about 0.3 shown in figure 4(a) is

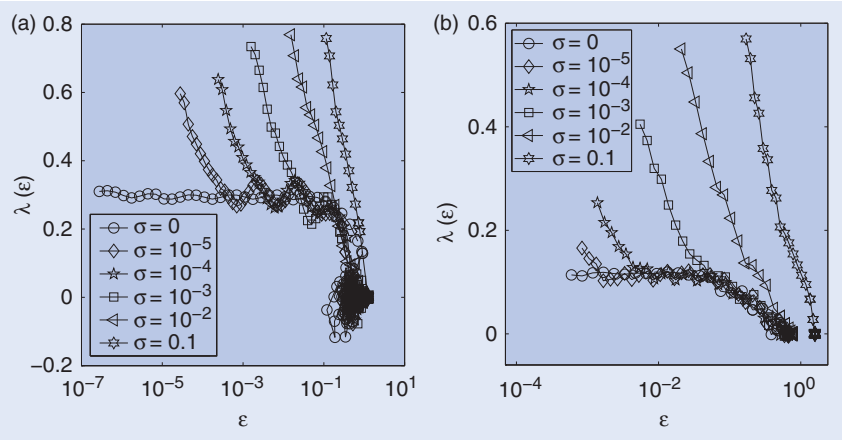

Figure 4. $\lambda(\epsilon)$ curves for the clean and the noisy asset pricing model with (a) the HM parameter set and (b) the BH parameter set.

larger than the value of the LE obtained by Hommes and Manzan (2006) using the neural network based LE estimator (as well as the algorithm of Wolf *et al.* 1985). We shall explain the reason for this discrepancy momentarily. (ii) The scale range where $\lambda(\epsilon)$ is almost constant is much wider for the HM parameter set than for the BH parameter set. In fact, only 10,000 points were used to calculate figure 4(a), while 30,000 points were used for figure 4(b). The reason for this is that the correlation dimension (Grassberger and Procaccia 1983a) for the chaotic attractor of the HM parameter set is only about 0.4, while that of the BH parameter set is about 2.0. This means that in order to resolve the behavior of $\lambda(\epsilon)$ on ever smaller scales, longer and longer time series have to be used. More precisely, for a given dataset, if the smallest resolvable scale is ϵ_0, in order to resolve a smaller scale ϵ_0/r, where $r>1$, a larger dataset has to be used—the larger the dimension of the attractor, the longer the time series has to be. (iii) When there is stochastic forcing, $\lambda(\epsilon)$ is no longer a constant when ϵ is small, but increases as $-\gamma \ln \epsilon$ when the scale ϵ is decreased. The coefficient γ does not seem to depend much on the strength of the noise. This feature suggests that entropy generation is infinite when $\epsilon \to 0$. (iv) When noise is increased, the part of the curve with $\lambda(\epsilon) \sim -\gamma \ln \epsilon$ shifts to the right, and the plateau region (i.e. $\lambda(\epsilon) \sim$ constant) shortens. Since the plateau region is a signature of chaos, we observe that a small chaotic signature can be identified when σ is increased beyond 0.01 for either parameter set.

We are now ready to understand how the LE λ_1 calculated by Hommes and Manzan (2006) using the neural network and the algorithm of Wolf *et al.* (1985) may be smaller than our estimate in the noise-free case. We first examine Wolf *et al.*'s algorithm. To monitor the exponential divergence between a reference and a perturbed trajectory, the algorithm of Wolf *et al.* (1985) employs a scale parameter ϵ^*. Whenever the divergence between a reference and a perturbed trajectory exceeds ϵ^*, a renormalization procedure is performed. When the algorithm of Wolf *et al.* (1985) is applied to a time series of finite length, in order to obtain a well-defined LE, a fairly large ϵ^* is typically chosen. Using equations (7) and (8), we then see that the discrepancy between our estimate and that of Hommes and Manzan is because the ϵ^* value used by them is larger than the scales where $\lambda(\epsilon)$ is almost constant.

Next, we examine the neural network based LE estimator. Here, the LE is estimated by the Jacobian matrix method (Eckmann and Ruelle 1985). The main function of the neural network is to estimate a trajectory in the phase space so that the Jacobian matrices can be computed. In estimating the trajectory in the phase space, a global optimization is employed, such that the error between the given time series and the estimated one is minimized. Global optimization involves a scale parameter. Hommes and Manzan's analysis suggests that this scale parameter is comparable to ϵ^* used by the algorithm of Wolf *et al.* (1985).

We are now ready to understand how LE estimated by a neural network or Wolf *et al.*'s algorithm may be negative in the strong noise case. To understand better, let us first use an intuitive argument. Suppose we have a noisy time series. After embedding, we can calculate the distances between two arbitrary points in the state space. Denote the most probable distance (which may be close to the mean distance) by D^*. Now if we take two points, X_i and X_j, whose distance $\|X_i - X_j\|$ is much smaller than D^*, then when time t goes by, on average the distance between X_{i+t} and X_{j+t} will increase with time rapidly until approaching D^*. This is divergence! Such a divergence remains when some suitable average is taken. Although this divergence may not be exponential (and thus not chaotic), the LE will be positive! Now, when can the LE be negative? It is when the distance between two initial points is already greater than $D*$. These arguments can be made more precise in the framework of SDLE, using the concept of the characteristic scale or limiting scale, ϵ_∞, defined by $\lambda(\epsilon_\infty) \sim 0$. If one starts from $\epsilon_0 \ll \epsilon_\infty$, then, regardless of whether the data are deterministically chaotic or simply random, ϵ_t will initially increase with time and gradually settle around ϵ_∞. Consequentially, $\lambda(\epsilon_t)$ will be positive before ϵ_t reaches ϵ_∞. On the other hand, if one starts from $\epsilon_0 \gg \epsilon_\infty$, then ϵ_t will simply decrease, yielding negative $\lambda(\epsilon_t)$, again regardless of whether the data are chaotic or random. When $\epsilon_0 \sim \epsilon_\infty$, then $\lambda(\epsilon_t)$ will stay around 0. Now, observing figures 4(a) and (b) again, we note that when noise is strong, the smallest scales that can be resolved by a finite dataset are always close to ϵ_∞. In order for an algorithm to numerically return a non-null result, the chosen scale parameter, such as ϵ^* of Wolf *et al.*'s algorithm, has to be larger than ϵ_∞. Since the probabilities for large scales are much larger than for small scales, equation (7) then means that the estimated LE is negative. Therefore, such a negative LE only indicates converging dynamics on large scales, but not the absence of diverging or noisy chaotic dynamics on small scales.

3.2. *The generalized Mackey–Glass model*

An interesting emerging paradigm for varying variance is the generalized Mackey–Glass (MG) model (Kyrtsou 2005, 2008, Dagum and Giannerini 2006), which may produce quite divergent dynamics depending on the values of its parameters; for example, the model may switch between chaotic and totally stochastic regions. It is interesting to examine what kind of chaotic dynamics the model is capable of generating. For this purpose, we examine the model proposed by Kyrtsou (2005). It reads

$$R_t = X_t + Y_t + \epsilon_t, \tag{18}$$

where

$$X_t = \alpha \frac{X_{t-\tau}}{1 + X_{t-\tau}^c} - \delta X_{t-1} \tag{19}$$

and

$$Y_t = b Y_{t-j}(1 - Y_{t-j}), \tag{20}$$

where $c=2$, $\alpha=2.1$ and $\delta=0.05$. Two cases were considered by Kyrtsou (2005): (i) $\tau=j=1$, $b=3.8$ and (ii) $\tau=j=5$, $b=4$. It is clear that the model is a superposition of the Mackey–Glass equation, the logistic equation, and noise. Here, noise is 'measurement', not dynamical, in the sense that noise is not in the iterations of the maps. In fact, it is easy to check that the system would diverge to infinity quickly were the noise dynamical. Note that the three components are not coupled.

We have studied the stability of the model and found that when $\tau=1$, the model has two stable fixed points, $x^*=\pm 1$; when $\tau=5$, while $x^*=\pm 1$ are still stable fixed point solutions, the model also allows other stable attractors, such as period-5 oscillations, depending on the initial conditions. However, there is no chaos in the Mackey–Glass equation. Therefore, the basic nonlinear chaotic dynamics of the generalized MG model are produced by the logistic equation, but not by the Mackey-Glass equation. The property of varying variance is thus produced by multiple stable attractors generated by the MG model; noise and the logistic equation amount to varying the initial conditions so that different stable attractors of the MG model can be realized.

3.3. *Analysis of US foreign exchange rate data*

Now that we have understood that an estimated negative LE may not imply the absence of noisy chaos in a noisy economic model, let us examine whether real economic time series may be characterized by noisy chaos. As example applications we analyse the US foreign exchange rate data downloaded from www.federalreserve.gov/releases/h10/hist/. In total, we have analysed 20 datasets, each with a sampling time of one day. Three examples are shown in figures 5(a1), (b1) and (c1), for US-Canada, US-Mexico, and US-Korea exchange rate data. The SDLE curves of figures 5(a2), (b2), and (c2) do not suggest the scalings of equations (9) and (10), therefore the dynamics are neither like deterministic chaos nor like noisy chaos. Instead, we observe that foreign exchange rate data are like random-walk-type processes, and are well characterized by equation (11), with the Hurst parameter taking all three types of values (close to, smaller than, and larger than 1/2 in figures 5(a2), (b2), and (c2), respectively). Of the 20 datasets, $H\approx 1/2$ is the most prevailing, as can be seen from table 1.

When estimating the Hurst parameter, it is important to check the consistency of an estimator. In our earlier studies, we found that, of the many estimators for the Hurst parameter, detrended fluctuation analysis (DFA) is a more flexible and more reliable method (Gao *et al.* 2006c, 2007). Furthermore, we have shown that multifractal-DFA is closely related to the singular measure based multifractal formalism and can readily characterize random cascade multifractals (Hu *et al.* 2009). We thus choose DFA to check the consistency of the SDLE-based H estimator.

When starting from a random walk of length N, DFA works as follows: (i) divide the random walk into $[N/m]$ non-overlapping segments (where the notation $[x]$ denotes

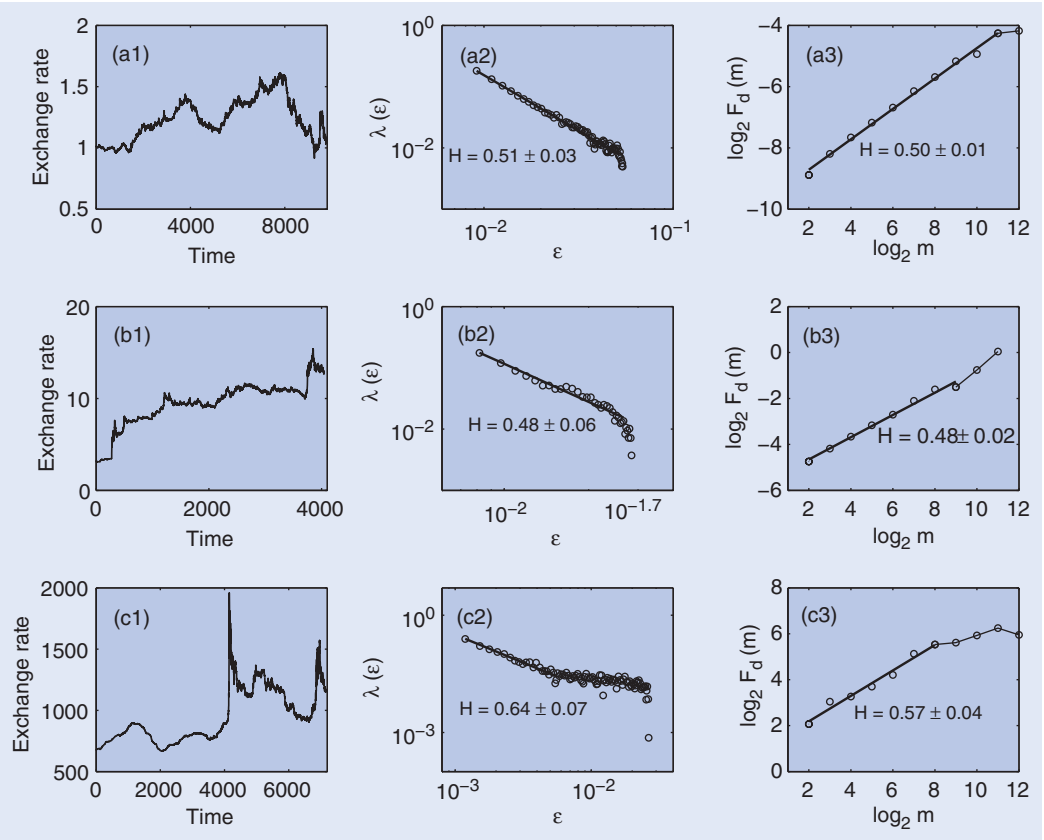

Figure 5. Foreign exchange rate data between the US and (a1) Canada, (b1) Mexico, and (c1) Korea. (a2,b2,c2) and (a3,b3,c3) are the corresponding SDLE $\lambda(\epsilon)$ and DFA ($\log_2 F_d(m)$ vs. $\log_2 m$) curves.

the largest integer that is not greater than x); (ii) define the local trend in each segment to be the ordinate of a linear least-squares fit for the random walk in that segment; and (iii) compute the 'detrended walk', denoted by $y_m(n)$, as the difference between the original walk $y(n)$ and the local trend. Then one examines

$$F_d(m) = \left\langle \sum_{i=1}^{m} y_m(i)^2 \right\rangle^{1/2} \sim m^H, \tag{21}$$

where the angled brackets denote the ensemble average of all the segments and $F_d(m)$ is the average variance over all segments. Figures 5(a3), (b3), and (c3) show the corresponding DFA curves for the three foreign exchange rate data examined by SDLE. We observe well-defined fractal scalings from DFA. The H values of other datasets have also been estimated by DFA and are listed in table 1. We observe that the H values estimated by SDLE are fully consistent with those estimated by DFA.

It is interesting to note that figure 5(c2) appears to have two scaling regimes. To determine what may have caused such behavior, we partition the data shown in figure 5(c1) into two parts where it jumps abruptly (which is around 4100), and calculate the SDLE and DFA curves for the two parts separately. The results are shown in figure 6. Comparing figure 6(a) with figure 5(c2), we observe that the first scaling regime is the common feature of both segments of the data, while the second scaling regime mainly comes from the first part of the data. However, this two-scaling behavior is not properly resolved by the DFA curves shown in figure 6(b). While the discussion

Table 1. The 20 exchange rate datasets analysed in this study; each dataset has a sampling time of one day.

Exchange rate data	Time span	Data Length	H estimated from SDLE	H estimated from DFA
EXALUS	1971 Jan 4–2009 Dec 14	9771	0.52 ± 0.03	0.50 ± 0.01
EXAUUS	1971 Jan 4–1998 Dec 31	7013	0.50 ± 0.04	0.49 ± 0.01
EXBEUS	1971 Jan 4–1998 Dec 31	7021	0.56 ± 0.02	0.54 ± 0.01
EXBZUS	1995 Jan 2–2009 Dec 14	3760	0.57 ± 0.04	0.55 ± 0.02
EXCAUS	1971 Jan 4–2009 Dec 14	9784	0.51 ± 0.03	0.50 ± 0.01
EXDNUS	1971 Jan 4–2009 Dec 14	9777	0.55 ± 0.04	0.52 ± 0.01
EXFRUS	1971 Jan 4–1998 Dec 31	7021	0.58 ± 0.06	0.54 ± 0.01
EXGEUS	1971 Jan 4–1998 Dec 31	7021	0.57 ± 0.04	0.54 ± 0.01
EXIRUS	1971 Jan 4–1998 Dec 31	7021	0.50 ± 0.04	0.51 ± 0.01
EXITUS	1971 Jan 4–1998 Dec 31	7020	0.52 ± 0.05	0.52 ± 0.01
EXJPUS	1971 Jan 4–2005 Oct 21	8728	0.53 ± 0.02	0.54 ± 0.01
EXKOUS	1981 Apr 13–2009 Dec 14	7162	0.64 ± 0.07	0.57 ± 0.04
EXMAUS	1971 Jan 4–2009 Dec 14	9756	0.53 ± 0.03	0.52 ± 0.01
EXMXUS	1993 Nov 8–2009 Dec 14	4046	0.48 ± 0.06	0.48 ± 0.02
EXNEUS	1971 Jan 4–1998 Dec 31	7021	0.60 ± 0.05	0.55 ± 0.01
EXNOUS	1971 Jan 4–2009 Dec 14	9777	0.52 ± 0.04	0.51 ± 0.01
EXNZUS	1971 Jan 4–2009 Dec 14	9762	0.50 ± 0.02	0.50 ± 0.01
EXSDUS	1971 Jan 4–2009 Dec 14	9777	0.48 ± 0.03	0.50 ± 0.01
EXSZUS	1971 Jan 4–2009 Dec 14	9778	0.50 ± 0.02	0.52 ± 0.01
EXUKUS	1971 Jan 4–2009 Dec 14	9778	0.55 ± 0.02	0.53 ± 0.01

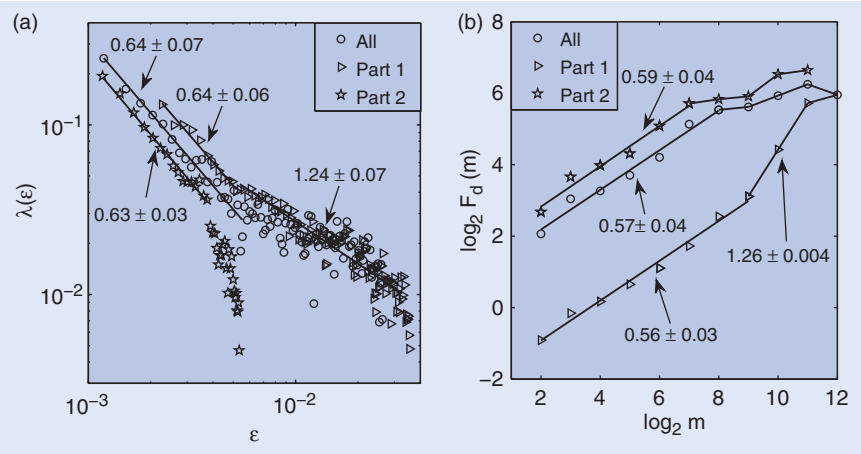

Figure 6. (a) SDLE ($\lambda(\epsilon)$ vs. ϵ) and (b) DFA ($\log_2 F_d(m)$ vs. $\log_2 m$) curves for foreign exchange rate data between the US and Korea. Black circles (and fitted lines), entire data set; green circles (and fitted lines), the first segment of the data; red circles (and fitted lines), second part of the data.

here clearly indicates that the two-scaling behavior is an intrinsic property of the data, it also signifies that SDLE can readily deal with non-stationarity.

Note that the foreign exchange rate data analysed here, when analysed by other H estimators, all yield consistent H values, just like the case of switching times in ambiguous visual perception (Gao *et al.* 2006a). We thus conclude that foreign exchange rate data are like random processes with a well-defined Hurst parameter.

4. Concluding remarks

To effectively characterize economic time series with complex behavior such as nonlinearity, non-stationarity, and fractal long-memory, we have proposed a SDLE-based multiscale analysis of financial data. SDLE not only unambiguously distinguishes low-dimensional chaos from noise, but also readily detects high-dimensional and intermittent chaos and aptly deals with certain types of non-stationarity (including dealing with outliers in real data without pre-processing). To examine the relevance of chaos to economic time series, we have analysed a noisy chaotic asset pricing model as well as 20 foreign exchange rate datasets. From the asset pricing model, we found that the negative largest LE estimated by a neural network estimator or by Wolf *et al.*'s algorithm (Hommes and Manzan 2006) may correspond to large-scale convergence, but does not imply the absence of small-scale divergence or noisy chaos. In fact, on small scales, divergence not only exists, but is also faster than truly chaotic dynamics. Therefore, the reported negative largest LE (Hommes and Manzan 2006) is an artifact of the specific algorithm used, and not an intrinsic property of noisy chaotic financial models. From foreign exchange rate data analysis, we found that while foreign exchange rate data are not chaotic, they nevertheless possess fractal scaling behavior, often characterized by a Hurst parameter very close to 1/2. Exceptions do arise occasionally, with H able to be either smaller or larger than 1/2.

Recall that the basic model for $H = 1/2$ is the standard Brownian motion, which is the foundation of the efficient market hypothesis. Therefore, H smaller or larger than 1/2 may be associated with deviations from the efficient market hypothesis. However, as far as the daily foreign exchange rate is concerned, the deviation from an efficient market is rather small, since even when H is smaller or larger than 1/2, the difference between H and 1/2 is not that large. Our discussions here are, however, cursory and somewhat speculative. To gain more insights into this issue, much more work needs to be done.

Acknowledgments

The authors thank Professors Yenn-Ru Chen and Sheng-Kwang Hwang at the National Chung Cheng University of Taiwan for many useful discussions. This work is partially supported by NSF grants CMMI-0825311 and 0826119.

References

Barnett, W.A., Comments on 'Chaotic monetary dynamics with confidence'. *J. Macroecon.*, 2006, **28**, 253–255.

Barnett, W.A. and Chen, P., The aggregation-theoretic monetary aggregates are chaotic and have strange attractors. In *An Econometric Application of Mathematical Chaos, Dynamic Econometric Modeling*, edited by W.A. Barnett, E. Berndt, and H. White, pp. 199–245, 1988 (Cambridge University Press: Cambridge).

Barnett, W.A., Gallant, A.R., Hinich, M.J., Jungeilges, J.A., Kaplan, D.T. and Jensen, M.J., A single-blind controlled competition among tests for nonlinearity and chaos. *J. Econometr.*, 1997, **82**, 157–192.

Breidt, F.J., Crato, N. and de Lima, P., The detection and estimation of long memory in stochastic volatility. *J. Econometr.*, 1998, **83**, 325–348.

Brock, W.A. and Hommes, C.H., Heterogeneous beliefs and routes to chaos in a simple asset pricing model. *J. Econ. Dynam. Control*, 1998, **22**, 1235–1274.

Brock, W.A. and Sayers, C.L., Is the business cycle characterized by deterministic chaos? *J. Monet. Econ.*, 1988, **22**, 71–90.

Dacorogna, M.M., Gencay, R., Muller, U., Olsen, R.B. and Pictet, O.V., *An Introduction to High-Frequency Finance*, 2001 (Academic Press: New York).

Dagum, E.B. and Giannerini, S., A critical investigation on detrending procedures for non-linear processes. *J. Macroecon.*, 2006, **28**, 175–191.

Di Matteo, T., Multi-scaling in finance. *Quant. Financ.*, 2007, **7**, 21–36.

Eckmann, J.-P. and Ruelle, D., Ergodic theory of chaos and strange attractors. *Rev. Mod. Phys.*, 1985, **57**, 617–656.

Gao, J.B., Chen, C.C., Hwang, S.K. and Liu, J.M., Noise-induced chaos. *Int. J. Mod. Phys. B*, 1999a, **13**, 3283–3305.

Gao, J.B., Hwang, S.K. and Liu, J.M., When can noise induce chaos? *Phys. Rev. Lett.*, 1999b, **82**, 1132–1135.

Gao, J.B., Billock, V.A., Merk, I., Tung, W.W., White, K.D., Harris, J.G. and Roychowdhury, V.P., Inertia and memory in ambiguous visual perception. *Cogn. Process.*, 2006a, **7**, 105–112.

Gao, J.B., Hu, J., Tung, W.W. and Cao, Y.H., Distinguishing chaos from noise by scale-dependent Lyapunov exponent. *Phys. Rev. E*, 2006b, **74**, 066204.

Gao, J.B., Hu, J., Tung, W.W., Cao, Y.H., Sarshar, N. and Roychowdhury, V.P., Assessment of long range correlation in time series: how to avoid pitfalls. *Phys. Rev. E*, 2006c, **73**, 016117.

Gao, J.B., Cao, Y.H., Tung, W.W. and Hu, J., *Multiscale Analysis of Complex Time Series—Integration of Chaos and Random Fractal Theory, and Beyond*, 2007 (Wiley: New York).

Gao, J.B. and Zheng, Z.M., Direct dynamical test for deterministic chaos and optimal embedding of a chaotic time series. *Phys. Rev. E*, 1994, **49**, 3807–3814.

Granger, C.W.J., Developments in the nonlinear analysis of economic series. *Scand. J. Econ.*, 1991, **93**, 263–276.

Granger, C.W.J., Is chaotic economic theory relevant for economics? A review article of: Jess Benhabib: Cycles and chaos in economic equilibrium. *J. Int. Compar. Econ.*, 1994, **3**, 139–145.

Granger, C.W.J. and Ding, Z.X., Varieties of long memory models. *J. Econometr.*, 1996, **73**, 61–77.

Grassberger, P. and Procaccia, I., Characterization of strange attractors. *Phys. Rev. Lett.*, 1983a, **50**, 346–349.

Grassberger, P. and Procaccia, I., Estimation of the Kolmogorov entropy from a chaotic signal. *Phys. Rev. A*, 1983b, **28**, 2591–2593.

Hommes, C.H. and Manzan, S., A comment on 'Testing for nonlinear structure and chaos in economic time series'. *J. Macroecon.*, 2006, **28**, 169–174.

Hu, J., Gao, J.B. and Wang, X.S., Multifractal analysis of sunspot time series: the effects of the 11-year cycle and Fourier truncation. *J. Statist. Mech.*, 2009, **02**, P02066.

Hwang, K., Gao, J.B. and Liu, J.M., Noise-induced chaos in an optically injected semiconductor laser. *Phys. Rev. E*, 2000, **61**, 5162–5170.

Kyrtsou, C., Evidence for neglected linearity in noisy chaotic models. *Int. J. Bifurc. Chaos*, 2005, **15**, 3391–3394.

Kyrtsou, C., Re-examining the sources of heteroskedasticity: the paradigm of noisy chaotic models. *Physica A*, 2008, **387**, 6785–6789.

Kyrtsou, C. and Serletis, A., Univariate tests for nonlinear structure. *J. Macroecon.*, 2006, **28**, 154–168.

Lorenz, E.N., Predictability: a problem partly solved. *Proceeding of a Seminar on Predictability*, pp. 1–18, 1996 (ECMWF: Reading, UK).

Lorenz, E.N., Designing chaotic models. *J. Atmos. Sci.*, 2005, **62**, 1574–1587.

Lorenz, E.N. and Emanuel, K.A., Optimal sites for supplementary weather observations: simulation with a small model. *J. Atmos. Sci.*, 1998, **55**, 399–414.

Mcmillan, D.G. and Speigh, A.E.H., Long-memory in high-frequency exchange rate volatility under temporal aggregation. *Quant. Finance*, 2008, **8**, 251–261.

Oswiecimka, P., Kwapien, J. and Drozdz, S., Multifractality in the stock market: price increments versus waiting times. *Physica A*, 2005, **347**, 626–638.

Packard, N.H., Crutchfield, J.P., Farmer, J.D. and Shaw, R.S., Geometry from a time series. *Phys. Rev. Lett.*, 1980, **45**, 712–716.

Pesin, Y.B., Characteristic Lyapunov exponents and smooth ergodic theory. *Russ. Math. Surv.*, 1977, **32**, 55–114.

Ruelle, D., *Thermodynamic Formalism*, 1978 (Addison-Wesley–Longman: Reading, MA).

Sauer, T., Yorke, J.A. and Casdagli, M., Embedology. *J. Statist. Phys.*, 1991, **65**, 579–616.

Scheinkman, J. and LeBaron, B., Nonlinear dynamics and stock returns. *J. Business*, 1989, **62**, 311–337.

Serletis, A. and Shintani, M., Chaotic monetary dynamics with confidence. *J. Macroecon.*, 2006, **28**, 228–252.

Shintani, M. and Linton, O., Is there chaos in the world economy? A nonparametric test using consistent standard errors. *Int. Econ. Rev.*, 2003, **44**, 331–358.

Shintani, M. and Linton, O., Nonparametric neural network estimation of Lyapunov exponents and a direct test for chaos. *J. Econometr.*, 2004, **120**, 1–33.

Takens, F., Detecting strange attractors in turbulence. In *Dynamical Systems and Turbulence*, *Lecture Notes in Mathematics*, *Vol. 898*, edited by D.A. Rand and L.S. Young, p. 366, 1981 (Springer: New York).

Wesner, N., Searching for chaos on low frequency. *Econ. Bull.*, 2004, **3**, 1–8.

Whang, Y.J. and Linton, O., The asymptotic distribution of nonparametric estimates of the Lyapunov exponent for stochastic time series. *J. Econometr.*, 1999, **91**, 1–42.

Wolf, A., Swift, J.B., Swinney, H.L. and Vastano, J.A., Determining Lyapunov exponents from a time series. *Physica D*, 1985, **16**, 285.

Zumbach, G., Volatility processes and volatility forecast with long memory. *Quant. Finance*, 2004, **4**, 70–86.